

1,3-DIGLYCERIDE-RICH EDIBLE OILS FROM GLYCEROLYSIS OF VEGETABLE OILS. EFFECT OF THE CATALYST BASIC PROPERTIES

L.A. DOSSO, P.J. LUGGREN and J.I. DI COSIMO

*Grupo de Investigación en Ciencias e Ingeniería Catalíticas (GICIC), Instituto de Investigaciones en Catálisis y Petroquímica (INCAPE), UNL-CONICET. Colectora Ruta Nacional 168, km 0, Paraje El Pozo (3000), Santa Fe, Argentina.
dicosimo@fiq.unl.edu.ar*

Abstract— Vegetable edible oils enriched in diglycerides were obtained by glycerolysis under heterogeneous catalysis conditions using MgO as catalyst. These oils contain up to 32wt.% of the 1,3-diglyceride isomer, which is believed to present unique nutritional properties to prevent obesity, compared to triglycerides or 1,2-diglycerides. The base site density and strength distribution of the different sites (weak, medium and strong) present on MgO as well as the initial oil conversion rate depend on the preparation procedure. The density of medium-strength sites increases upon increasing the severity of the preparation procedure in the range of 673-873K in parallel to the initial oil conversion rate. These results confirm that medium-strength base sites promote the kinetically relevant reaction steps involved in the glycerolysis of vegetable oils.

Keywords— triglycerides; diglycerides; glycerolysis; base catalysis; MgO.

I. INTRODUCTION

In the last decades the food industry has been making important efforts for the release to the market of healthier food products (Maki *et al.*, 2002; Murase and Kimura, 2004).

Vegetable oils are mainly triesters of glycerol known as triacylglycerols (triglycerides, TAG) containing acyl chains coming from oleic, linoleic, linolenic, palmitic and stearic fatty acids. The regular intake of vegetable oils may result in weight gain, body fat accumulation and the consequent related diseases. On the other hand, diglycerides (DAG) are diesters of glycerol containing two acyl chains; they are minor components of oils. DAG exist in two isomeric forms, the asymmetric sn-1,2-diglyceride (1,2-DAG) and the symmetric sn-1,3-diglyceride (1,3-DAG) which follow different metabolic pathways in the small intestine. Whereas TAG and 1,2-DAG are converted by hydrolysis into free fatty acids (FFA) and 2-monoglycerides (2-MAG) which eventually are transformed back to TAG, the 1,3-DAG isomer is hydrolyzed to 1-MAG and FFA, thereby avoiding both, formation of the 2-MAG intermediate and re-synthesis of TAG with the resulting fat deposit in the body tissues.

Therefore, consumption of an oil enriched in 1,3-DAG may have beneficial effects to prevent obesity and associated health issues (Gotoh and Shimasaki, 2004).

Few previous works report the use of solid basic catalysts to promote the glycerolysis of the TAG present in

oils, aiming to obtain either a mixture of MAG and DAG (Corma *et al.*, 1998) or a DAG-rich oil (Zhong *et al.*, 2014). Recently, we studied the synthesis of vegetable oils enriched specifically in 1,3-DAG by glycerolysis of the oil with glycerol (Gly) using MgO as a solid base catalyst (Ferretti *et al.*, 2018). We found that MgO efficiently promotes the reaction and that the total DAG and the 1,3-DAG contents depend on the operational conditions such as reaction temperature and Gly/TAG reactant ratio, among others.

Time ago, we reported how the MgO basic properties (base site density and strength distribution) can be tuned by properly choosing the solid preparation conditions. We also explained how a change in those basic properties affects the kinetics of the monoglyceride synthesis by glycerolysis of fatty acid methyl esters with glycerol (Bellelli *et al.*, 2015).

However, there are no reports in the literature about the basicity requirements for the vegetable oil glycerolysis reaction. Thus, in this work we continue our investigations on the base-catalyzed synthesis of 1,3-DAG-rich vegetable oils with the aim to elucidate how the MgO preparation conditions affect the solid textural and basic properties as well as the catalyst activity and product distribution. By changing the solid synthesis conditions, we identify the chemical nature of the MgO base sites participating in the reaction kinetics.

II. METHODS

A. Catalyst Synthesis and Characterization

Magnesium oxide was prepared from commercial MgO (Sigma Aldrich $\geq 99\%$) by hydration with distilled water to obtain Mg(OH)₂ which was then decomposed back to MgO in a N₂ flow. Samples were stabilized at that 673, 773 or 873K for 18h. Details are given elsewhere (Ferretti *et al.*, 2018). Another set of MgO samples was prepared by treating commercial MgO at the same 3 temperatures but without previous hydration. After thermal treatment the resulting MgO samples were ground and sieved, and the particles with average particle size of 177-250 μm were used for the catalytic experiments.

The MgO textural properties such as BET surface area (SA) and pore volume (PV) were measured by N₂ physisorption at 77 K in a NOVA-1000 Quantachrome sorptometer. The MgO structural properties were investigated by powder X-ray diffraction (XRD) analysis; a Shimadzu XD-D1 diffractometer equipped with Cu-K α radiation source ($\lambda = 0.1542 \text{ nm}$) was used.

The basic properties of the MgO catalysts were measured by temperature-programmed desorption (TPD) of CO₂. MgO samples were exposed at room temperature to a flowing mixture of 3 % of CO₂ in N₂ until reaching surface saturation. After CO₂ adsorption, weakly adsorbed CO₂ was removed by flushing the reactor with a flow of N₂. Then, the temperature was increased to 773 K at a ramp rate of 10 K/min to desorb chemically bonded CO₂. The CO₂ concentration in the N₂ flow at the reactor exit was monitored with a flame ionization detector after converting CO₂ into CH₄ on a methanation catalyst (Ni/Kieselghur).

B. Glycerolysis Reaction

The glycerolysis of vegetable oils with glycerol was carried out at 493 K in a seven-necked cylindrical glass reactor equipped mechanical stirring. Commercial sunflower cooking oil (Molinos Río de la Plata S.A.) purchased from a local supermarket was used as a source of triglycerides (TAG). Oil and refined glycerol (Sigma-Aldrich, 99.8%) were loaded in the reactor with a Gly/TAG molar ratio of 0.8. The reactor was operated at atmospheric pressure in a batch regime for the liquid phases. A continuous flow of N₂ (70 mL/min) was used to maintain an inert atmosphere inside the reactor and to remove water. The liquid mixture was heated to the reaction temperature under stirring at 700 rpm and then the solid catalyst was added to start the reaction. The proper amount of MgO solid catalyst (W_{MgO}) was pretreated ex-situ overnight in a N₂ stream at the corresponding stabilization temperature (673, 773 or 873K) and then kept at 373K in a N₂ flow until utilization. Oil conversion (X_{TAG}), was calculated as

$$X_{TAG} (\%) = \frac{n_{TAG}^0 - n_{TAG}}{n_{TAG}^0} \times 100$$

where n_{TAG}^0 and n_{TAG} are the moles of oil at $t=0$ and $t=t$, respectively.

C. Analysis of Glycerides, Fatty Acid Profile and Free Fatty Acids

Eleven samples of the reaction mixture were extracted at specific reaction times during the 8h catalytic run. All reactions were conducted in duplicate. The data points in figures are the mean value of samples extracted at the same reaction time during the duplicated runs. Samples were centrifuged at room temperature (3000rpm) and the supernatant oily phase was analyzed by HPLC. Mono, di and triglycerides were quantified in a Shimadzu LC-10A liquid chromatograph (Shimadzu Corp.) equipped with a quaternary pump system, an on-line degasser, a 20 μ L sample loop, column oven (323K), and a spectrophotometer with UV visible detector ($\lambda = 210$ nm). A 150 x 3.9 mm ID reversed-phase analytical column C18 (μ Bondapak C18, Waters) was used. Two mobile phases were used (mobile phase A: acetonitrile:methanol (4:1 V/V); mobile phase B: n-hexane:2-propanol (8:5 V/V)). Solvent flow rate and oven temperature were selected as 0.7 mL/min and 323K, respectively (Ferretti *et al.*, 2018).

The fatty acid profile of the oil before and after glycerolysis was determined after converting the samples to fatty acid methyl esters (FAME) by transesterification with methanol. Then, samples were analyzed by gas chromatography (GC) in a 7890A Agilent Technologies GC equipped with a FID detector and a Supelcowax-10 30M capillary column (Ferretti *et al.*, 2018). Previous calibration was carried out using standard solutions of the main FAME present in the fresh oil. The fatty acids were coded as (m:n) where m is the carbon length of the acyl chain and n is the number of unsaturations. In sunflower oil, palmitic (16:0), stearic (18:0), oleic (18:1) and linoleic (18:2) acids were identified.

Oleic acid (Sigma-Aldrich $\geq 99\%$) was used as standard for calibration in the quantification of free fatty acids. Analyses were performed in the fresh oil and in the oily phase at the end of the 8h catalytic runs or at other reaction times using a modified Lowry and Tinsley method (Lowry and Tinsley, 1976; Ferretti *et al.*, 2018). A UV-Vis Lambda 40 spectrophotometer (Perkin-Elmer) set at 700 nm was used.

III. RESULTS AND DISCUSSION

A. Catalyst Characterization

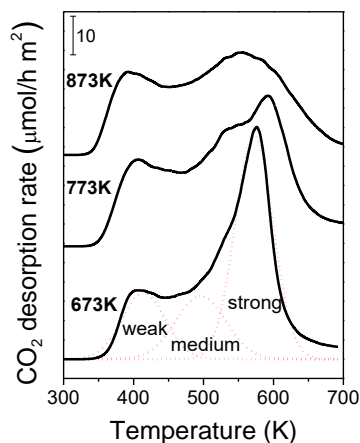
MgO converts to Mg(OH)₂ (brucite) after hydration. Thermal decomposition of brucite precursors at 673-873K leads to formation of high surface area (SA) MgO oxides. Also, the SA and pore size values of the materials prepared by this procedure were higher than those of the MgO samples treated at the same temperatures but without hydration. It seems that removal of structural water molecules as gaseous H₂O during brucite decomposition generates an enhanced porosity. Large catalyst pores are needed in the glycerolysis reaction to fit the long TAG of the oil. In addition, when the MgO samples without previous transformation to brucite were tested in the glycerolysis reaction, the resulting enriched oil presented a dark color and a high FFA content. Thus, the chemical transformation of MgO to brucite and of the latter back to MgO probably removes oxide impurities that generate undesirable products that affect the final product quality. Thus, hereinafter only results obtained with hydrated MgO samples will be discussed.

Table 1 presents the physicochemical properties of MgO samples hydrated and treated at different stabilization temperatures. Results show that after increasing the severity of the thermal treatment both, SA and PV decrease due to sintering of the porous structure. Coalescence of small pores explains the larger mean pore size calculated with the Wheeler equation (Pore size = $4 \cdot 10^4$ PV/SA).

In previous works we have investigated the basic properties of similar MgO catalysts by adsorbing at room temperature an acid probe molecule such as CO₂ and using a combination of FTIR (Fourier-transform infrared spectroscopy) and TPD techniques (Beelli *et al.*, 2015). We found that CO₂ is adsorbed on surface oxygen species of different coordination and chemical nature. At least three different CO₂ adsorption species were identified:

Table 1. Textural and basic properties of MgO samples hydrated and treated at different stabilization temperatures.

T (K)	SA (m ² /g)	PV (cm ³ /g)	Pore size (Å)	Base site density (μmol/m ²)			
				total	weak	medium	strong
673	88	0.25	114	11.7	2.4	2.5	6.8
773	52	0.22	169	12.5	2.3	4.3	5.9
873	44	0.18	164	11.1	1.9	4.6	4.6

Fig. 1. CO₂ TPD profiles of MgO catalysts hydrated and treated at different stabilization temperatures

unidentate carbonate, bidentate carbonate and bicarbonate. Unidentate carbonate formation requires low-coordination O²⁻ anions, such as those present at corners or edges (O_{3c} or O_{4c}). Bidentate carbonate forms on high-coordination acid-base pairs (Mg_{5c} - O_{5c}), abundant on surface terraces. Both carbonates can be detected by FTIR after evacuation at increasing temperatures, but only the unidentate species remain on the surface after evacuation at or above 473K. On the other hand, formation of bicarbonate species involves surface hydroxyl groups but these species disappear after evacuation at 373K due to the weak basic nature of the surface OH⁻ groups of MgO. Thus, the following base strength order was proved for these surface oxygen species: low coordination O²⁻ anions > oxygen in Mg²⁺ - O²⁻ pairs > OH⁻ groups.

Here, Fig. 1 shows the CO₂ TPD results for the MgO samples treated at three different temperatures. By integration of the TPD traces, the total base site density in μmol/m² was calculated. The TPD profiles were deconvoluted in three peaks to quantify the contribution of weak (OH⁻ groups), medium-strength (oxygen in Mg²⁺ - O²⁻ pairs of high coordination number) and strong (coordinatively unsaturated O²⁻ anions) base sites, Table 1. Although the total base site density was similar irrespective of the stabilization temperature, the contribution of each base site was notoriously dependent on the thermal treatment. Thus, the density of medium-strength sites increases at higher temperatures at the expense of that of the strong sites. An explanation for this result is that upon increasing the severity of the treatment, surface defects (O_{3c} or O_{4c} species) responsible for the strong basicity, disappear. Thus, the MgO surface becomes smoother enhancing the contribution of high coordination number O²⁻

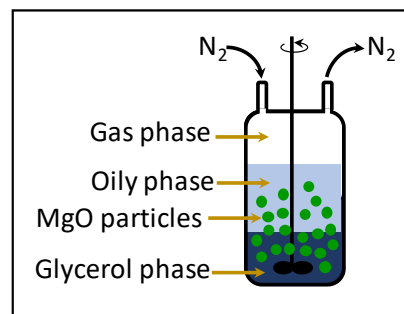


Fig. 2. Four-phase reactor for glycerolysis of vegetable oils.

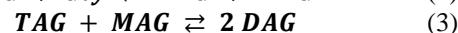
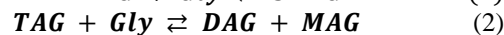
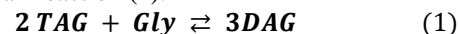
ions such as those in terraces (Mg_{5c} - O_{5c} pairs). Furthermore, MgO surface hydroxylation, i.e., the contribution of OH⁻ groups, decreases at high stabilization temperatures, in agreement with previous results (Belelli *et al.*, 2015).

The overall result is that the thermal treatment during MgO preparation procedures affects the oxide average basicity. Solid stabilization at high temperatures reduces not only the surface hydroxylation but also the density of strong sites as a result of the partial elimination of coordinatively unsaturated oxygen anions, giving rise to less basic oxides.

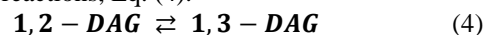
B. Heterogeneously-Catalyzed Glycerolysis

The glycerolysis of vegetable oils was carried under heterogeneous catalysis conditions using the four-phase reactor depicted in Fig. 2. Two immiscible liquid layers (oily and glycerol phases), the solid catalyst phase and the inert gas phase participate in the glycerolysis process.

The reaction under study is presented in Eq. (1). However, we have shown that it takes place in steps (Ferretti, *et al.*, 2018). At low conversions the TAG of the oil react with Gly according to Eq. (2) to give equimolar amounts of DAG and MAG. But at higher conversion levels, the consecutive reaction between TAG and the intermediate MAG occurs, generating two more molecules of DAG, Eq. (3). The combination of Eq. (2) and (3) gives the overall reaction (1).



Since the purpose of this work is to enrich the oil in 1,3-DAG, it is relevant to investigate the possible occurrence of acyl migration processes such as isomer interconversion reactions, Eq. (4).



The oil is not soluble in Gly but the latter is just slightly soluble in the oil. Therefore, the set of reactions (1)-(4) takes place in the upper layer, to where Gly has to be transferred under vigorous stirring.

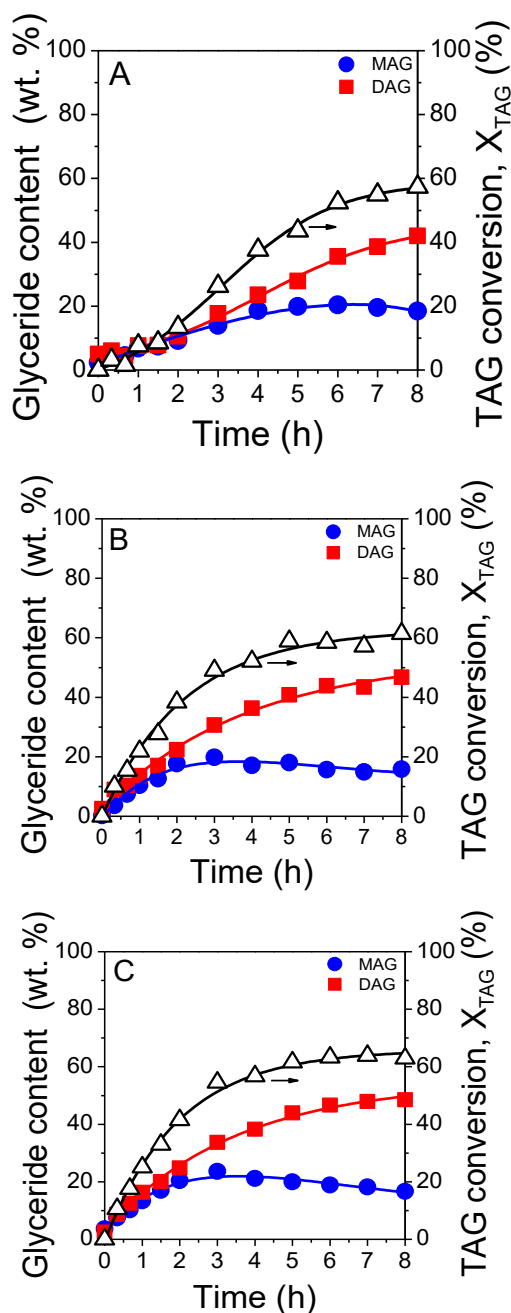


Fig. 3. Time evolution of the heterogeneously catalyzed glycerolysis reaction. MAG and DAG content and TAG conversion on MgO hydrated and treated at different stabilization temperatures. A: 673K; B: 773K and C: 873K. [sunflower oil, refined glycerol, $T = 493\text{K}$, $\text{Gly}/\text{TAG} = 0.8$ (molar ratio), $W_{MgO}/n_{TAG}^0 = 9\text{ g/mol}$, $70\text{ mL N}_2/\text{min}$].

C. Effect of the MgO Preparation Conditions on the Glycerolysis

Figure 3 presents the time evolution of the catalytic results of the glycerolysis of sunflower oil using MgO catalysts treated at stabilization temperatures of 673, 773 and 873K. The only glyceride products detected in the course of reaction were DAG and MAG. The shape of the curves in Fig. 3 is consistent with reaction steps (2) and (3). At the beginning of the reaction almost equal amounts of MAG and DAG form, indicating that both are primary products of the glycerolysis reaction, Eq. (2). At higher reaction times, the maximum in the MAG curve agrees with the consecutive conversion of MAG in DAG by Eq. (3). DAG were the dominant products at the end of the runs ($\text{DAG}/\text{MAG} > 2$) because the Gly/TAG ratio employed in the catalytic experiments is close to the stoichiometric ratio of the overall reaction (1). We discussed before (Ferretti *et al.*, 2018) that higher Gly/TAG ratios shift the reaction sequence toward undesirable reactions, such as (5).



Fresh sunflower oil contains 97.4 wt.% TAG, 0.6 wt.% MAG and 2.0 wt.% DAG with a FFA acid content of 0.14 wt. % and Table 2 shows changes in oil composition after glycerolysis. In all cases, X_{TAG} values close to equilibrium conditions ($\sim 60\%$) were reached before the end of the 8-hour run. However, a slight increase of X_{TAG} ($\sim 63\%$) at MgO stabilization temperatures of 773-873K was observed (Fig. 3), as well as enhanced total DAG ($\sim 48\%$) and 1,3-DAG ($\sim 32\%$) contents, Table 2. The DAG content increases at high temperatures at the expense of MAG, as indicated by the DAG/MAG ratio. Thus, the thermal treatment of MgO at high temperatures favors step (3). Contrarily, the 1,3-DAG/1,2-DAG ratio was around 2 during the entire 8-hour catalytic run regardless of the MgO activation conditions. This result was observed before for glycerolysis under other conditions (Ferretti *et al.*, 2018) suggesting that also under the present experimental conditions, reaction (4) is equilibrated and shifted to the right from the beginning. Furthermore, the FFA content was much lower when MgO was treated at high temperatures in agreement with the lower catalyst surface hydroxylation. Traces of water molecules on the surface of MgO catalysts would promote the undesirable oil hydrolysis with formation of FFA that might affect oil quality and catalyst stability.

Figure 4 presents the time evolution of 1,3-DAG showing that main changes in curve shape and final value occur after increasing the MgO stabilization temperature

Table 2. Composition of sunflower oil after glycerolysis on MgO hydrated and treated at different temperatures

T (K)	Composition (wt.%) ^a										
	Fatty acid distribution				Glyceride content						
	16:0 ^b	18:0 ^c	18:1 ^d (ω -9)	18:2 ^e (ω -6)	MAG	DAG	TAG	1,3-DAG	$\frac{\text{DAG}}{\text{MAG}}$	$\frac{1,3\text{-DAG}}{1,2\text{-DAG}}$	FFA
673	6.2	3.4	42.1	48.3	18.5	42.0	39.5	28.5	2.3	2.1	4.0
773	6.3	3.4	42.3	48.0	15.8	46.7	37.5	31.5	3.0	2.1	1.6
873	6.2	3.4	42.1	48.3	16.6	48.5	34.8	31.7	2.9	1.9	1.6

^a after the 8h-reaction at 493K with Gly/TAG=0.8, without any further purification treatment; ^b palmitic; ^c stearic; ^d oleic; ^e linoleic

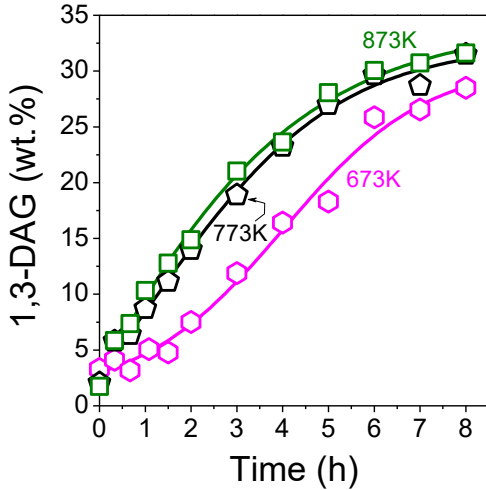


Fig. 4. Time evolution of the 1,3-DAG content on MgO hydrated and treated at stabilization temperatures of 673, 773 and 873K. Conditions as in Fig.3.

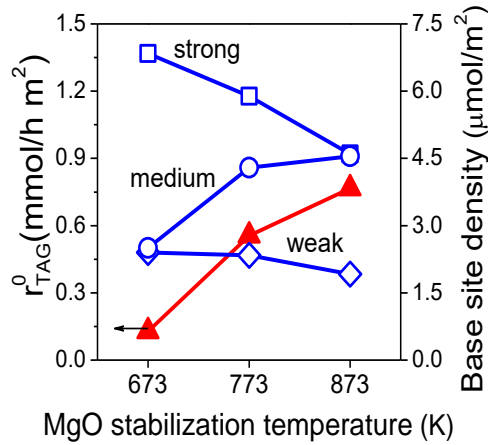


Fig. 5. Effect of MgO stabilization temperature on the initial reaction rate and base site density distribution.

from 673 to 773K. A further increase to 873K slightly enhances the final 1,3-DAG content.

D. Kinetic Aspects. Active Site Identification

As can be seen in the time evolution of the catalytic results of Fig. 3, the overall reaction is faster as the MgO stabilization temperature increases, as suggested by the increasing initial slope of the X_{TAG} versus time curves. To quantify this effect, calculations of the initial TAG conversion rates (r_{TAG}^0 , mmol/h m²) were carried out from the slopes at $t=0$, according to Eq. (6) and plotted in Fig. 5 as a function of the MgO stabilization temperature.

$$r_{TAG}^0 = \left(\frac{n_{TAG}^0}{SA W_{MgO}} \right) \times \left(\frac{dX_{TAG}}{dt} \right)_{t=0} \quad (6)$$

External and internal mass transfer limitations (m.t.l.) were ruled out after calculations of the Mears (ω) and Weisz-Prater (Φ) criteria, respectively, using the r_{TAG}^0 values of Fig. 5 (Mears, 1971; Weisz and Prater, 1954; Ferretti *et al.*, 2018). Values of ω in the range of 3.33×10^{-3} - 9.94×10^{-3} were calculated assuming a reaction order of 1; these values are lower than 0.15 which is the limit postulated by the criterion to have external m.t.l.

Similarly, assuming first order reactions and spherical particles the calculated Φ values of 0.057-0.171 correspond to Thiele moduli of 0.058-0.131 and effectiveness factors of 0.999-0.994, confirming the absence of internal m.t.l. Thus, the r_{TAG}^0 values of Fig. 5 were obtained under kinetic regime.

In Fig. 5, the r_{TAG}^0 plot was superimposed to the base site density distribution (weak, medium and strong sites, Table 1). Clearly, the kinetic results follow a trend similar to that of the density of intermediate strength base sites since both parameters increase with the severity of the MgO thermal treatment. In fact, a plot relating both parameters gives a straight line (not shown), suggesting that these sites participate in kinetically relevant reaction steps. In a previous work on glycerolysis of methyl oleate (a fatty acid methyl ester, FAME), on similar MgO catalysts, we found a linear correlation between activity and the density of strong sites (Belelli *et al.*, 2015). Thus, the present results suggest, instead, that glycerolysis of vegetable oils is less demanding of basicity compared with that of FAME.

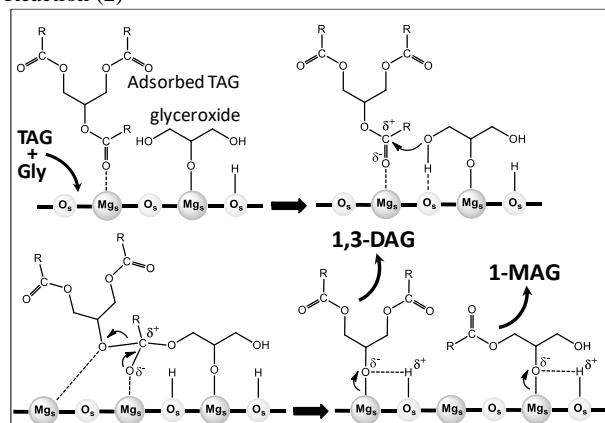
Scheme 1 postulates simplified versions of the surface reactions (2) and (3) on MgO based on our previous experience on other transesterification reactions (Belelli *et al.*, 2015). For reaction step (2), after Gly approaches the MgO surface, a surface glyceroxide and a proton species are formed by dissociative Gly adsorption on a surface Mg-O pair (Mg_s-O_s). On the other hand, TAG contains three acyl chains (R-C=O) at positions 1, 2, and 3 of the glycerol backbone. TAG is associatively adsorbed on a Mg_s through the C=O function at position 2. One H is then abstracted from the OH group of the glyceroxide species by an O_s giving a surface proton whereas the oxygen of glyceroxide attacks the adjacently adsorbed TAG. Then, a new C-O bond forms between the two adsorbed molecules, after which a C-O bond belonging to the TAG molecule breaks giving rise to 1,3-diglyceroxide and 1-monoglyceroxide surface molecules. They further react with surface hydrogen fragments to be released to the liquid phase as 1,3-DAG and 1-MAG. If the TAG molecule were adsorbed through the C=O function at position 1, the final outcome would be formation of the 1,2-DAG isomer and 1-MAG.

A similar mechanism applies for reaction step (3) between an adsorbed TAG and a 1-monoglyceroxide. The final result is formation of two molecules of 1,3-DAG. If the attack of the 1-monoglyceroxide species were at position 1 of the TAG molecule, the result of reaction step (3) would be one 1,2-DAG and one 1,3-DAG.

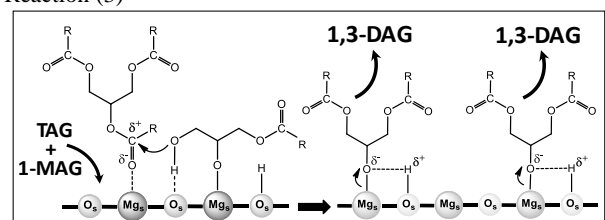
IV. CONCLUSIONS

The MgO stabilization temperature affects the distribution of base sites. At higher temperatures, strong sites assigned to coordinatively unsaturated oxygen anions disappear giving rise to smoother surfaces containing an enhanced contribution of medium strength sites. With increasing the severity of the thermal treatment, the initial reaction rate parallels the trend of the medium strength sites. Therefore, these sites mainly promote the reaction.

Reaction (2)



Reaction (3)



Scheme 1: Simplified surface reaction pathway for reactions steps (2) and (3). [R-C=O: acyl chains from palmitic, stearic, oleic or linoleic acids]

Using MgO catalysts activated at 673-873K, TAG conversions $\geq 60\%$ were obtained after reaction at 493K. The best results were obtained on MgO catalysts with a proper combination of basic sites such as those treated at 773-873K. On these materials, equilibrium conditions were reached in 5h and the resulting modified oils contain $\sim 48\%$ of total DAG and $\sim 32\%$ of 1,3-DAG with a low FAA content.

ACKNOWLEDGEMENTS

Authors thank the Agencia Nacional de Promoción Científica y Tecnológica (ANPCyT), Argentina (grant PICT 1217/14), CONICET, Argentina (grant PUE 22920160100106CO/16) for financial support of this work. They also thank Dr C.A. Ferretti and M.L. Spotti for the development of the analytical techniques.

REFERENCES

Belelli, P.G., Ferretti, C.A., Apesteguía, C.R., Ferullo, R.M. and Di Cosimo, J.I. (2015). "Glycerolysis of methyl oleate on MgO: Experimental and theoretical study of the reaction selectivity," *J. Catal.* **323**,

132-144.

Corma, A., Iborra, S., Miquel, S. and Primo, J. (1998). "Production of food emulsifiers, monoglycerides, by glycerolysis of fats with solid base catalysts," *J. Catal.*, **173**, 315-321.

Ferretti, C.A., Spotti, M.L. and Di Cosimo, J.I. (2018). "Diglyceride-rich oils from glycerolysis of edible vegetable oils," *Catal. Today*, **302**, 233-241.

Gotoh, N. and Shimasaki, H. (2004). "Suppressive effects of diacylglycerol oil on postprandial serum triglyceride elevation in animals," *Diacylglycerol Oils*. T. Katsuragi, N. Yasukawa, B.D. Matsuo, I. Flickinger, M.G. Tokimitsu (Eds.), AOCS Press, Champaign, 70-76.

Lowry, R.R. and Tinsley, I.J. (1976). "Rapid Colorimetric Determination of Free Fatty Acids," *J. Am. Oil Chem. Soc.*, **7**, 470-472.

Maki, K.C., Davidson, M.H., Tsushima, R., Matsuo, N., Tokimitsu, I., Umporowicz, D.M., Dicklin, M.R., Foster, G.S., Ingram, K.A., Anderson, B.D., Frost, S.D. and Bell, M. (2002). "Consumption of diacylglycerol oil as part of a reduced-energy diet enhances loss of body weight and fat in comparison with consumption of a triacylglycerol control oil," *Am. J. Clin. Nutr.*, **76**, 1230-1236.

Mears, D.E., "Tests for transport limitations in experimental catalytic reactors", *Ind. Eng. Chem. Proc. Des. Develop.*, **10** (4), 438-447(1971).

Murase, T. and Kimura, S. (2004). "Activation of lipid metabolism and energy expenditure by dietary diacylglycerol," *Diacylglycerol Oils*, T. Katsuragi, N. Yasukawa, B.D. Matsuo, I. Flickinger, M.G. Tokimitsu (Eds.), AOCS Press, Champaign, 46-57.

Weisz, P.B. and Prater, C.D. (1954). "Interpretation of Measurements in Experimental Catalysis," *Adv. Catal.*, **6**, 143-196.

Zhong, N., Deng, X., Huang, J., Xu, L., Hu, K. and Gao, Y. (2014) "Low-temperature chemical glycerolysis to produce diacylglycerols by heterogeneous base catalyst," *Eur. J. Lipid Sci. Technol.*, **116**, 470-476.

Received October 25, 2019

Sent to Subject Editor October 30, 2019

Accepted January 15, 2019

Recommended by Editor-in-Chief:

J. Alberto Bandoni